Supplementary information

S1) Additional method explanation

S1.1) Cell-wise runoff using the curve number method

The cell-wise runoff depth (R_{CN}) of eq. (5) in the main manuscript text was calculated using the Soil Conservation Service Curve Number method (SCS-CN) method. An in-depth overview of the theory behind the curve number example can be found in (Hawkins et al., 2008), and several examples of its integration with RUSLE to predict gross and/or net erosion are available (e.g. Gao et al., 2012; Mishra et al., 2006). Runoff (R_{CN}) is calculated via:

$$R_{CN} = \frac{(P - I_a)^2}{P - I_a + S}, \quad \text{(S.1)}$$

Where P is the event precipitation (mm) of each RUSLE event, I_a is the initial abstraction (mm), and S is the potential maximum retention (mm), given by:

$$S = \frac{(P - I_a)^2}{P - I_a + S}, \quad \text{(S.2)}$$

I_a was set to 0 for the simulation cases since water discharge and sediment yield were known to have been produced at the catchment outlet. The curve number (CN) is a dimensionless variable assigned to each land use depending on the hydrological soil group, soil hydrological condition and antecedent moisture condition. The CN numbers were assigned according to the tabular values presented in Hawkins et al., (2008) for the different land use types (Table. S1).

Table S1: The applied initial curve number used for the different land use classes utlised in the study. The 'WorldCover classification' column gives the landcover classification according to the ESA WorldCover layer (Zanaga et al., 2022) and 'CN table land use' gives the corresponding assigned names from the CN lookup table (Hawkins et al., 2008).

WorldCover classification	CN table land use	Treatment or practice	Physical intervention	Hydrological condition	CN (AMC 2)
Cropland	Fallow	Straight row	0		86
Cropland	Row Crops	Straight row	0	Poor	81
Cropland	Row Crops	Straight row	0	Good	78
Cropland	Small grain	Straight row	0	Poor	76

Cropland	Small grain	Straight row	0	Good	75
Grassland/Shrubland	Pasture or range		0	Good	61
Grassland/Shrubland	Pasture or range		0	Poor	67
Tree cover	Meadow Woods		0	Poor	66
Tree cover	Meadow Woods		0	Good	55
Path	Dirt roads		0		82
Built-up	Asphalt roads		0		84
River	Water body		0		100

At each pixel, a 'poor' vs 'good' hydrological condition based on a soil loss ratio above or below 0.4 respectively. Cropland areas with an soil loss ratio (SLR) > 0.7 during an event were attributed the CN class of 'Fallow'. Furthermore, the antecedent moisture condition (AMC) values are known to be a key factor determining the event specific runoff response to a rainfall event. To scale between three AMC classes for each land use category, the normalised antecedent precipitation index (NAPI) was used:

$$NAPI = \frac{\sum_{t=-1}^{-T} P_t k^{-t}}{\bar{P} \sum_{t=-1}^{-T} k^{-t}}, \quad \text{(S.3)}$$

As applied in Hong et al., (2007). Where T = 5 days, P is the daily precipitation, $\bar{P}$ is the average daily precipitation, and k is a decay constant with the value of 0.85. Daily precipitation was taken from the gridded European Meterological Observations (EMO) dataset at roughly 1 km grid resolution to ensure a representative average (Thiemig et al., 2022). NAPI thresholds of < 0.33 and > 3 represent the 'dry' and 'wet' AMC conditions respectively, while intermediate values define the 'fair' condition and given the CN_2 value (Table. S1). For dry and wet AMC conditions, the scaling equations formulae, as described by Hawkins et al., (2008) and applied in Hong et al., (2007) were used:

$$CN_1 = \frac{CN_2}{2.281 - 0.01281\, CN_2}, \quad \text{(S.4)}$$

$$CN_3 = \frac{CN_2}{0.427 - 0.00573\, CN_2}, \quad \text{(S.5)}$$

S1.2) Calculating the event-scale EI30 index

Gauge measurements for each catchment time series data was processed into discrete EI30 events based on the RUSLE definition (Wischmeier & Smith, 1978):

$$EI30 = \left(\sum_{r=1}^{0} e_r v_r\right) I_{30}, \quad \text{(S.6)}$$

In which vr is the rainfall depth per event (mm), I30 is the maximum 30-minute rainfall intensity during the event (mm h^{-1}), and e_r is the unit rainfall energy ($MJha^{-1}mm^{-1}$) calculated via the equation utilised by (Verstraeten et al., 2006) for Central Belgium:

$$e_r = 11.12 i_r^{1.31}, \quad \text{(S.7)}$$

Where i_r is the rainfall intensity of the event (mm h^{-1}). Typically a minimum threshold for the event rainfall depth is set at 12.7 mm, or 6.35 mm during a period of 15 minutes or less. Although considered to have a minor overall difference on the total erosivity (Lu & Yu, 2002). Accordingly, all events exceeding 1.27 mm were considered as potentially erosive, and thereafter periods of erosive rainfall were matched with periods of runoff and sediment transport in the monitored channel network.

The rainfall records in all catchments were resampled to 10 minute resolution before the calculating the discrete EI30 events. An open source Python implementation of the Verstraeten et al., (2006) algorithm was used for all catchments (https://pypi.org/project/rfactor/).

S1.3) A further description of temporally-static input parameters

A selection of parameter layers necessary for the model run were considered temporally static and processed using an automated Python procedure for the catchment boundaries. These parameters include: The K-factor, the topographic grid, land cover, field parcel delineations, and road and path elements. For each simulated catchment in EUSEDcollab, a digital elevation model (DEM) was first extracted from the 25-metre resolution Copernicus EU-DEM for a bounding box exceeding the catchment extent. A flow direction algorithm was thereafter implemented on the grid to delineate the catchment upstream area from the registered catchment stream outlet coordinates for each catchment.

A geospatial alignment, overlaying and value reclassification process was implemented to prepare the model input layers within the model bounds. The land cover layer was generated by overlaying IACS field parcel data onto the 10-meter resolution WorldCover layer (Zanaga et al., 2022). WorldCover has the advantage of resolving spatial features at high resolution in comparison to the 100-meter resolution CORINE landcover layer for Europe. Additionally, roads and paths were added to the land cover grid from the Open Street Map (*OpenStreetMap*, 2023) portal and parameterised in the standard way (i.e. connecting elements in the landscape). The K-factor surface was taken from the European layer based on harmonised soil sampling through the LUCAS campaign (Orgiazzi et al., 2018; Panagos et al., 2014).

S1.4) Further processing of the multitemporal soil loss ratio (SLR)

Field parcel polygons from the Integrated Administrative Control System (IACS) were used to parameterise the landscape spatial elements in an object oriented manner (Borrelli et al., 2018; Efthimiou et al., 2022; Schneider et al., 2023). These elements comprise both the units for the SLR parameterisation and for defining the parcel connectivity elements in W/S. However, IACS data are modern compared to the time extent of some catchment data, therefore a buffered polygon of 30 m was first created around the parcel centroid point to mitigate the effects of changing field parcel structures over multiple years. Thereafter, the median NDVI pixel value within each centroid polygon was acquired for each Landsat image within the catchment measuring period plus an additional 2-year window buffer.

The original method of Matthews et al., (2022) considered a binary assessment of conventional vs conservation tillage to include the effect of crop residues on the SLR through time. However, given the relatively low recurrence frequency of Landsat, only the green canopy cover component of the C-factor was considered. In addition, the exact crop cultivation succession for each parcel across the analysis years is unknown, meaning that a unique crop-wise relationship between the NDVI and crop canopy cover could not be applied. We instead apply the general linear regression equation established by Tenreiro et al., (2021) for all compiled crop species.

S1.5) Multiple model simulation scenarios

Multiple model scenarios were run for two purposes: 1) to obtain the best performing connectivity parameters for each catchment in a systematic way, and 2) the determine the best transport capacity based on the presence of systematic changes in model performance across sediment delivery ratio limits. W/S has several additional parameters describing the cellular connectivity of sediment transport in the model. These include land-use interconnectivity (forest connectivity (FC), cropland connectivity (CC)), trapping efficiency (forest trapping efficiency (FTE), pasture trapping efficiency (PTE), cropland trapping efficiency (CTE)) and the stream network position. In most model applications these parameters are considered fixed, given that otherwise a higher parameter dimensionality is introduced into the calibration scheme. Yet several studies highlight the varying importance of these parameters in modifying the connectivity of sediment to stream channels (Batista et al., 2022). Moreover, parameters induce a high sensitivity in the model response which could impact W/S in a multi-temporal simulation mode. In determining the best possible parameter set for the dynamic model implementation, we therefore ran the model simulation routine 100 times for each catchment. In each case, a parameter set was selected by random sampling across a parameter space of potential values before determining an 'optimum' parameter set. The multiple sub-parameters were thereafter compiled into a singular connectivity index:

$$CI = CC_R + FC_R + CTE_R + FTE_R + PTE_R + CIT_R, \quad (S.8)$$

In which each sub-parameter is the rank (R) between 0 and 1 of the sampled parameter from its prior range Table. (S2). Thereafter, the optimal ktchigh and ktclow values were determined for each connectivity scenario in the model calibration process.

Table. S2: The parameter limits used to define the extents of the multi-scenario model runs. Each model input value was randomly generated from an array of 10 values generated between the pre-defined parameter bounds. The Sediment Delivery Ratio (SDR) is defined as an intermediate parameter calculated before running the sediment delivery routine, representing the ratio of the measured suspended sediment yield (SSY) to the RUSLE gross erosion (ER) prediction.

Parameter name	Low value	High value
Cropland connectivity	80	100
Forest connectivity	10	50
Cropland trapping efficiency	0	20
Forest trapping efficiency	50	90
Pasture trapping efficiency	50	90
Channel initiation threshold	Initial value * 0.5	Initial value * 1.2

Sediment delivery ratio (SSY:ER)	Mean value	Maximum value

We secondly investigated changes in model efficiency as events exceeding a given sediment delivery ratio (SDR) threshold are removed. Per event, the SDR is calculated as:

$$SDR = \frac{SSY}{\sum ER_{cell}}, \quad \text{(S.9)}$$

Which is calculated by dividing the 15-day catchment sediment yield by the sum of the cell-wise gross erosion across the catchment. Based on this ratio between the RUSLE grid and measured sediment yield, a necessary sediment delivery ratio can be calculated prior to running the sediment delivery module (de Vente et al., 2008). High SDR values can represent events in which a large error is not caused by model error, but other phenomena such as: 1) a large error in their parameterisation (e.g. precipitation under-catch or an unrepresentative catchment SLR value), or 2) events in which erosion processes not simulated in W/S (e.g. gully incision or bank erosion) were dominant. To investigate the model response to varying event compositions, we then investigate the model performance as the upper SDR threshold is varied incrementally between the mean and maximum.

S2) Additional results

The rate of loss in model performance as the SDR limit was increased showed differences across the different TC formulae, indicating varying abilities to simulate the full spectrum of events. For this reason, slightly better model performances occurred when events exceeding a certain SDR were omitted from the record : Ganspoel (NSE = 0.34, SDR_{limit} = 0.3) > Kinderveld (NSE = 0.13, SDR_{limit} = 0.07) > FDTL (NSE = 0.06, SDR_{limit} = 0.07) > BRVL (NSE = 0.04, SDR_{limit} = 0.02). Of the three tested transport capacity equations, only the S-A transport capacity produced a relatively consistent model performance across the full spectrum of SDR values (Fig. S1). The standard W/S transport capacity formulation tended to produce poorer model performances when the maximum SDR bound was increased, a case particularly evident in the Kinderveld catchment.

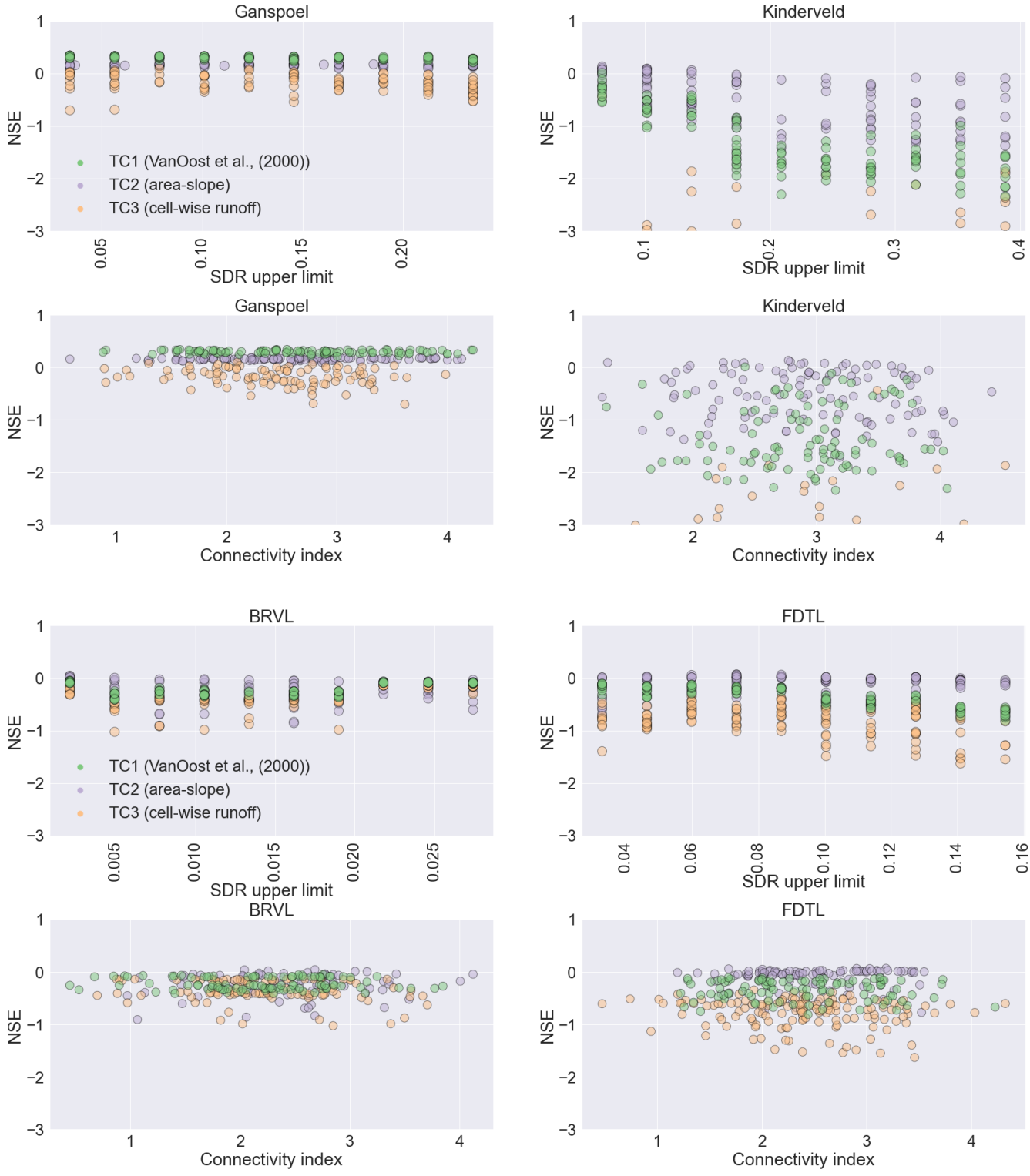
Ganspoel
Kinderveld
BRVL
FDTL
NSE
SDR upper limit
Connectivity index
TC1 (VanOost et al., (2000))
TC2 (area-slope)
TC3 (cell-wise runoff)

Figure S1: Plots per catchment showing the variation in the model performance (NSE) for different model parameter combinations and structural changes in the transport capacity equation (point colour). Upper panel in each plot: the NSE response to changes in the maximum permitted event sediment delivery ratio (SDR). The far right extent of each plot considers the entire aggregated sediment yield in each catchment (i.e. no limitation in the maximum SDR). Vertical spread derives from variation in the constituent sub-parameters within the 'connectivity index'. Lower panel in each plot: the NSE response to changes in the connectivity index. Vertical spread attributes to the sub-parameters in each 'connectivity index' value as well as the varying SDR thresholds in each model run.

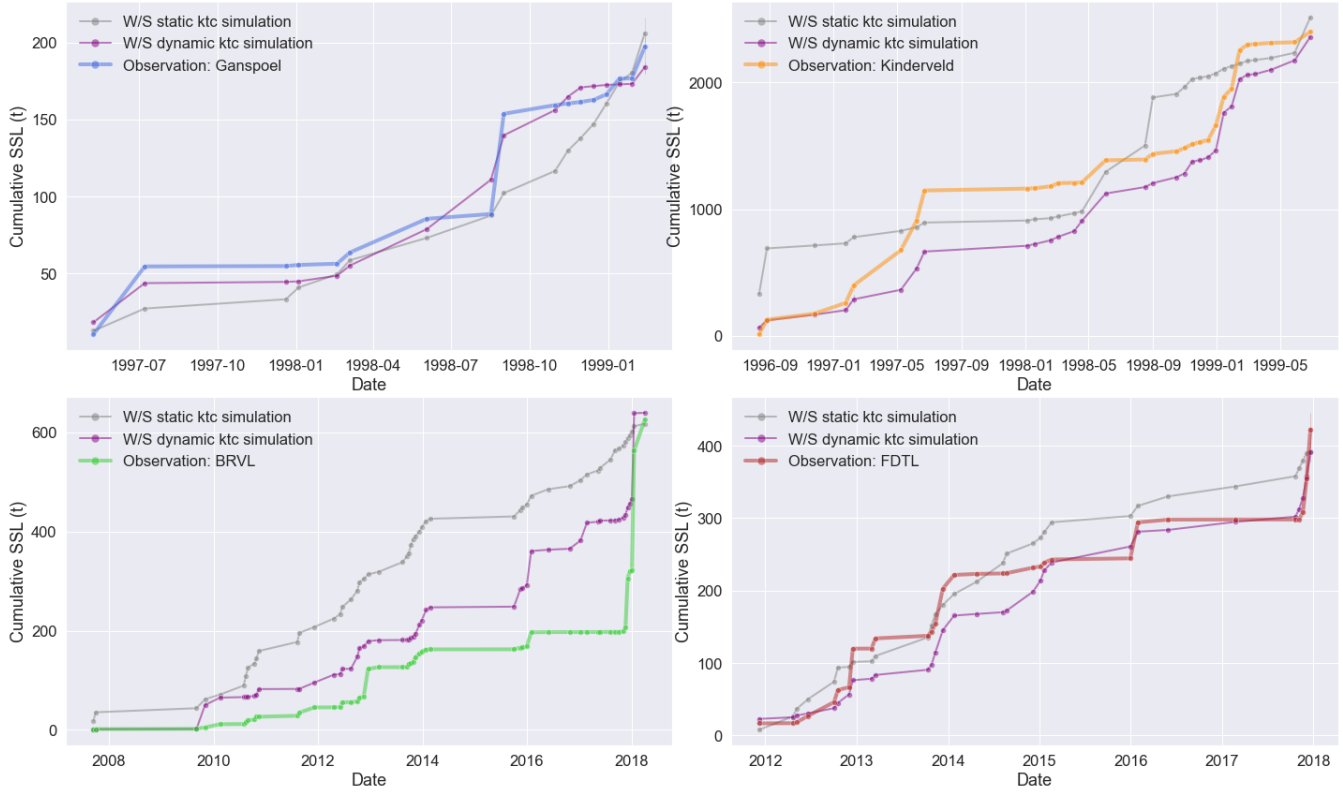

Figure S2: Cumulative sediment load plots comparing the 15-day sediment delivery for the temporally static and dynamic WaTEM/SEDEM implementations. A comparison is given for the Ganspoel (BE), Kinderveld (BE), BRVL (FR) and FDTL (BE) catchments respectively.

Supplementary references

Batista, P. V. G., Fiener, P., Scheper, S., & Alewell, C. (2022). A conceptual-model-based sediment connectivity assessment for patchy agricultural catchments. *Hydrology and Earth System Sciences*, *26*(14), 3753–3770. https://doi.org/10.5194/HESS-26-3753-2022

Borrelli, P., Meusburger, K., Ballabio, C., Panagos, P., & Alewell, C. (2018). Object-oriented soil erosion modelling: A possible paradigm shift from potential to actual risk assessments in agricultural environments. *Land Degradation and Development*, *29*(4), 1270–1281. https://doi.org/10.1002/ldr.2898

de Vente, J., Poesen, J., Verstraeten, G., Van Rompaey, A., & Govers, G. (2008). Spatially distributed modelling of soil erosion and sediment yield at regional scales in Spain. *Global and Planetary Change*, *60*(3–4), 393–415. https://doi.org/10.1016/j.gloplacha.2007.05.002

Efthimiou, N., Psomiadis, E., Papanikolaou, I., Soulis, K. X., Borrelli, P., & Panagos, P. (2022). A new high resolution object-oriented approach to define the spatiotemporal dynamics of the cover-management factor in soil erosion modelling. *CATENA*, *213*, 106149. https://doi.org/10.1016/J.CATENA.2022.106149

Gao, G. Y., Fu, B. J., Lü, Y. H., Liu, Y., Wang, S., & Zhou, J. (2012). Coupling the modified SCS-CN and RUSLE models to simulate hydrological effects of restoring vegetation in the Loess Plateau of China. *Hydrology and Earth System Sciences*, *16*(7), 2347–2364. https://doi.org/10.5194/HESS-16-2347-2012

Hawkins, R. H., Ward, T. J., Woodward, D. E., & Van Mullem, J. A. (2008). Curve Number Hydrology. *Curve Number Hydrology: State of the Practice*, 1–106. https://doi.org/10.1061/9780784410042

Hong, Y., Adler, R. F., Hossain, F., Curtis, S., & Huffman, G. J. (2007). A first approach to global runoff simulation using satellite rainfall estimation. *Water Resources Research*, *43*(8). https://doi.org/10.1029/2006WR005739

Lu, H., & Yu, B. (2002). Spatial and seasonal distribution of rainfall erosivity in Australia. *Soil Research*, *40*(6), 887–901. https://doi.org/10.1071/SR01117

Matthews, F., Verstraeten, G., Borrelli, P., & Panagos, P. (2022). A field parcel-oriented approach to evaluate the crop cover-management factor and time-distributed erosion risk in Europe. *International Soil and Water Conservation Research*. https://doi.org/10.1016/J.ISWCR.2022.09.005

Mishra, S. K., Tyagi, J. V., Singh, V. P., & Singh, R. (2006). SCS-CN-based modeling of sediment yield. *Journal of Hydrology*, *324*(1–4), 301–322. https://doi.org/10.1016/J.JHYDROL.2005.10.006

OpenStreetMap. (2023). https://www.openstreetmap.org/#map=8/50.510/4.475

Orgiazzi, A., Ballabio, C., Panagos, P., Jones, A., & Fernández-Ugalde, O. (2018). LUCAS Soil, the largest expandable soil dataset for Europe: a review. *European Journal of Soil Science*, *69*(1), 140–153. https://doi.org/10.1111/EJSS.12499

Panagos, P., Meusburger, K., Ballabio, C., Borrelli, P., & Alewell, C. (2014). Soil erodibility in Europe: A high-resolution dataset based on LUCAS. *Science of the Total Environment*, *479–480*(1), 189–200. https://doi.org/10.1016/j.scitotenv.2014.02.010

Schneider, M., Schelte, T., Schmitz, F., & Körner, M. (2023). EuroCrops: The Largest Harmonized Open Crop Dataset Across the European Union. *Scientific Data*, *10*(1), 612. https://doi.org/10.1038/s41597-023-02517-0

Tenreiro, T. R., García-Vila, M., Gómez, J. A., Jiménez-Berni, J. A., & Fereres, E. (2021). Using NDVI for the assessment of canopy cover in agricultural crops within modelling research. *Computers and Electronics in Agriculture*, *182*, 106038. https://doi.org/10.1016/J.COMPAG.2021.106038

Thiemig, V., Gomes, G. N., Skøien, J. O., Ziese, M., Rauthe-Schöch, A., Rustemeier, E., Rehfeldt, K., Walawender, J. P., Kolbe, C., Pichon, D., Schweim, C., & Salamon, P. (2022). EMO-5: a high-resolution multi-variable gridded meteorological dataset for Europe. *Earth System Science Data*, *14*(7), 3249–3272. https://doi.org/10.5194/ESSD-14-3249-2022

Verstraeten, G., Poesen, J., Demarée, G., & Salles, C. (2006). Long-term (105 years) variability in rain erosivity as derived from 10-min rainfall depth data for Ukkel (Brussels, Belgium): Implications for assessing soil erosion rates. *Journal of Geophysical Research*, *111*(D22), D22109. https://doi.org/10.1029/2006JD007169

Wischmeier, H., & Smith, D. D. (1978). Predicting Rainfall Erosion Losses: A Guide to Conservation Planning. In *United States Department of Agriculture*. Hyattsville, Md. (USA) US Dept. of Agriculture, Science and Education Administration. https://agris.fao.org/agris-search/search.do?recordID=XF2016064337

Zanaga, D., Van De Kerchove, R., Daems, D., De Keersmaecker, W., Brockmann, C., Kirches, G., Wevers, J., Cartus, O., Santoro, M., Fritz, S., Lesiv, M., Herold, M., Tsendbazar, N.-E., Xu, P., Ramoino, F., & Arino, O. (2022). *ESA WorldCover 10 m 2021 v200*. https://doi.org/10.5281/ZENODO.7254221